
Discriminative Entropy Clustering and its Relation to K-means and SVM

Anonymous Author(s)

Abstract

1 Maximization of mutual information between the model’s input and output is
2 formally related to “decisiveness” and “fairness” of the softmax predictions Bridle
3 et al. (1991), motivating such unsupervised entropy-based losses for discriminative
4 models. Recent self-labeling methods based on such losses represent the state of
5 the art in deep clustering. First, we discuss a number of general properties of such
6 entropy clustering methods, including their relation to K-means and unsupervised
7 SVM-based techniques. Disproving some earlier published claims, we point out
8 fundamental differences with K-means. On the other hand, we show similarity
9 with SVM-based clustering allowing us to link explicit margin maximization to
10 entropy clustering. Finally, we observe that the common form of cross-entropy is
11 not robust to pseudo-label errors. Our new loss addresses the problem and leads to
12 a new EM algorithm improving the state of the art on many standard benchmarks.

13 1 Introduction

14 Discriminative entropy-based loss functions, e.g. *decisiveness* and *fairness*, were proposed for
15 network training Bridle et al. (1991); Krause et al. (2010) and regularization Grandvalet & Bengio
16 (2004) and are commonly used for unsupervised and weakly-supervised classification problems
17 Ghasedi Dizaji et al. (2017); Hu et al. (2017); Ji et al. (2019); Asano et al. (2020); Jabi et al. (2021).
18 In particular, the state-of-the-art in unsupervised classification Asano et al. (2020); Jabi et al. (2021)
19 is achieved by self-labeling methods using extensions of decisiveness and fairness.

20 Section 1.1 reviews the entropy-based clustering with soft-max models and introduces the necessary
21 notation. Then, Section 1.2 reviews the corresponding self-labeling formulations. Section 1.3
22 summarizes our main contributions and outlines the structure of the main parts of the paper.

23 1.1 Discriminative entropy clustering: background and notation

24 Consider neural networks using probability-type outputs, e.g. *softmax* $\sigma : \mathcal{R}^K \rightarrow \Delta^K$ mapping
25 K logits $l^k \in \mathcal{R}$ to K -class probabilities $\sigma^k = \frac{\exp l^k}{\sum_c \exp l^c}$ forming a categorical distribution $\sigma =$
26 $(\sigma^1, \dots, \sigma^K) \in \Delta^K$ often interpreted as a posterior. We reserve superscripts to indicate classes or
27 categories. For shortness, this paper uses the same symbol for functions or mappings and examples of
28 their output, e.g. specific predictions σ . If necessary, subscript i can indicate values, e.g. prediction
29 σ_i or logit l_i^k , corresponding to any specific input example X_i in the training dataset $\{X_i\}_{i=1}^N$.

30 The *mutual information* (MI) loss, proposed by Bridle et al. (1991) for unsupervised discriminative
31 training of softmax models, trains the model output to keep as much information about the input
32 as possible. They derived MI estimate as the difference between the average entropy of the output
33 $\overline{H(\sigma)} = \frac{1}{N} \sum_i H(\sigma_i)$ and the entropy of the average output $\bar{\sigma} = \frac{1}{N} \sum_i \sigma_i$, which is a distribution of
34 class predictions over the whole dataset

$$L_{mi} := -MI(C, X) \approx \overline{H(\sigma)} - H(\bar{\sigma}) \quad (1)$$

35 where C is a random variable representing the class prediction for input X . Besides the motivating
 36 information-theoretic interpretation of the loss, the right-hand side in (1) has a clear discriminative
 37 interpretation that stands on its own: $H(\bar{\sigma})$ encourages “fair” predictions with a balanced support
 38 of all categories across the whole training dataset, while $\overline{H(\sigma)}$ encourages confident or “decisive”
 39 prediction at each data point suggesting that decision boundaries are away from the training examples
 40 Grandvalet & Bengio (2004). Our paper refers to unsupervised training of discriminative soft-max
 41 models using predictions’ entropies, e.g. see (1), as *discriminative entropy clustering*. This should
 42 not be confused with *generative entropy clustering* methods where the entropy is used as a measure
 43 of compactness for clusters’ density functions¹.

44 Discriminative clustering loss (1) can be applied to deep or shallow models. For clarity, this
 45 paper distinguishes parameters \mathbf{w} of the *representation* layers of the network computing features
 46 $f_{\mathbf{w}}(X) \in \mathcal{R}^M$ for any input X . We separate the linear classifier parameters \mathbf{v} in the output layer
 47 computing K -logit vector $l = \mathbf{v}^\top f$ for any feature $f \in \mathcal{R}^M$. As mentioned earlier, this paper uses
 48 the same notation for mapping $f(\cdot)$ and its values or (deep) features f produced by the representation
 49 layers. For shortness, we assume a “homogeneous” representation of the linear classifier so that $\mathbf{v}^\top f$
 50 includes the bias. The overall network model is defined as

$$\sigma(\mathbf{v}^\top f_{\mathbf{w}}(X)). \quad (2)$$

51 A special “shallow” case of the model in (2) is a basic linear discriminator

$$\sigma(\mathbf{v}^\top X) \quad (3)$$

52 directly operating on given input features $f(X) = X$. In this case, M represents the input dimensions.
 53 Optimization of the loss (1) for the shallow model (3) is done only over linear classifier parameters \mathbf{v} ,
 54 but the deeper network model (2) is optimized over all network parameters $[\mathbf{v}, \mathbf{w}]$. Typically, this is
 55 done via gradient descent or backpropagation Rumelhart et al. (1986); Bridle et al. (1991).

56 In the context of deep models (2), the decision boundaries between the clusters of data points $\{X_i\}$
 57 can be arbitrarily complex since the network learns high-dimensional non-linear representation map
 58 or embedding $f_{\mathbf{w}}(X)$. In this case, loss (1) is optimized with respect to both representation \mathbf{w} and
 59 classification \mathbf{v} parameters. To avoid overly complex clustering of the training data and to improve
 60 generality, it is common to use *self-augmentation* techniques Hu et al. (2017). For example, Ji et al.
 61 (2019) maximize the mutual information between class predictions for input X and its augmentation
 62 counterpart X' encouraging deep features invariant to augmentation.

63 To reduce the model’s complexity, Krause et al. (2010) combine entropy-based loss (1) with regular-
 64 ization of all network parameters interpreted as their isotropic Gaussian prior

$$\begin{aligned} L_{mi+decay} &= \overline{H(\sigma)} - H(\bar{\sigma}) + \|\mathbf{v}, \mathbf{w}\|^2 \\ &\stackrel{c}{=} \overline{H(\sigma)} + KL(\bar{\sigma} \| u) + \|\mathbf{v}, \mathbf{w}\|^2 \end{aligned} \quad (4)$$

65 where $\stackrel{c}{=}$ represents equality up to an additive constant and u is a uniform distribution over K classes.
 66 The second loss formulation in (4) uses KL divergence motivated in Krause et al. (2010) by the
 67 possibility to generalize the fairness to any target balancing distribution different from the uniform.

68 1.2 Self-labeling methods for entropy clustering

69 Optimization of losses (1) or (4) during network training is mostly done with standard gradient descent
 70 or backpropagation Bridle et al. (1991); Krause et al. (2010); Hu et al. (2017). However, the difference
 71 between the two entropy terms implies non-convexity, which makes such losses challenging for
 72 gradient descent. This motivates alternative formulations and optimization approaches. For example,
 73 it is common to extend the loss by incorporating auxiliary or hidden variables y representing *pseudo-*
 74 *labels* for unlabeled data points X , which are to be estimated jointly with optimization of the network
 75 parameters Ghasedi Dizaji et al. (2017); Asano et al. (2020); Jabi et al. (2021). Typically, such
 76 *self-labeling* approaches to unsupervised network training iterate optimization of the loss over pseudo-
 77 labels and network parameters, similarly to Lloyd’s algorithm for K -means or EM algorithm for
 78 Gaussian mixtures Bishop (2006). While the network parameters are still optimized via gradient
 79 descent, the pseudo-labels can be optimized via more powerful algorithms.

¹E.g., K-means minimizes cluster variances, whose logs are cluster’s density entropies, assuming Gaussianity.

80 For example, Asano et al. (2020) formulate self-labeling using the following constrained optimization
 81 problem with discrete pseudo-labels y tied to predictions by *cross entropy* function $H(y, \sigma)$

$$L_{ce} = \overline{H(y, \sigma)} \quad \text{s.t. } y \in \Delta_{0,1}^K \quad \text{and} \quad \bar{y} = u \quad (5)$$

82 where $\Delta_{0,1}^K$ are *one-hot* distributions, *i.e.* corners of the probability simplex Δ^K . Training of the
 83 network is done by minimizing cross entropy $H(y, \sigma)$, which is convex w.r.t. σ , assuming fixed
 84 pseudo-labels y . Then, model predictions get fixed and cross-entropy is minimized w.r.t variables
 85 y . Note that cross-entropy $H(y, \sigma)$ is linear with respect to y , and its minimum over simplex Δ^K
 86 is achieved by one-hot distribution for a class label corresponding to $\arg \max(\sigma)$ at each training
 87 example. However, the balancing constraint $\bar{y} = u$ converts minimization of cross-entropy over all
 88 data points into a non-trivial integer programming problem that can be approximately solved via
 89 *optimal transport* Cuturi (2013). The cross-entropy in (5) encourages the network predictions σ to
 90 approximate the estimated one-hot target distributions y , which implies the decisiveness.

91 Self-labeling methods for unsupervised clustering can also use soft pseudo-labels $y \in \Delta^K$ as
 92 target distributions inside $H(y, \sigma)$. In general, soft targets y are commonly used with cross-entropy
 93 functions $H(y, \sigma)$, e.g. in the context of noisy labels Tanaka et al. (2018); Song et al. (2022). Softened
 94 targets y can also assist network calibration Guo et al. (2017); Müller et al. (2019) and improve
 95 generalization by reducing over-confidence Pereyra et al. (2017). In the context of unsupervised
 96 clustering, cross entropy $H(y, \sigma)$ with soft pseudo-labels y approximates the decisiveness since it
 97 encourages $\sigma \approx y$ implying $H(y, \sigma) \approx H(y) \approx H(\sigma)$ where the latter is the decisiveness term in (1).
 98 Inspired by (4), instead of the hard constraint $\bar{y} = u$ used in (5), self-labeling losses can represent
 99 the fairness using KL divergence $KL(\bar{y} \| u)$, as in Ghasedi Dizaji et al. (2017); Jabi et al. (2021). In
 100 particular, Jabi et al. (2021) formulates the following entropy-based self-labeling loss

$$L_{ce+kl} = \overline{H(y, \sigma)} + KL(\bar{y} \| u) \quad (6)$$

101 encouraging decisiveness and fairness, as discussed. Similarly to (5), the network parameters in loss
 102 (6) are trained by the standard cross-entropy term. Optimization over relaxed pseudo-labels $y \in \Delta^K$
 103 is relatively easy since KL divergence is convex and cross-entropy is linear w.r.t. y . While there
 104 is no closed-form solution, the authors offer an efficient approximate solver for y . Iterating steps
 105 that estimate pseudo-labels y and optimize the model parameters resemble the Lloyd’s algorithm for
 106 K-means. Jabi et al. (2021) also establish a formal relation with K-means objective.

107 1.3 Summary of our contributions

108 Our work is closely related to self-labeling loss (6) and the corresponding ADM algorithm proposed
 109 in Jabi et al. (2021). Their inspiring approach is a good reference point for our self-labeling loss
 110 formulation (13). It also helps to illuminate the limits in a general understanding of entropy clustering.

111 Our paper provides conceptual and algorithmic contributions. First of all, we examine the relations of
 112 discriminative entropy clustering to K-means and SVM. In particular, we disprove the main theoretical
 113 claim (in the title) of a recent TPAMI paper Jabi et al. (2021) wrongly stating the equivalence between
 114 the standard K-means objective and the entropy-based clustering losses. Our Figure 1 provides a
 115 simple counterexample to the claim, but we also show specific technical errors in their proof. We
 116 highlight fundamental differences with a broader *generative* group of clustering methods, which
 117 includes K-means, GMM, etc. On the other hand, we find stronger similarities between entropy
 118 clustering and discriminative SVM-based clustering. In particular, this helps to formally show the
 119 soft margin maximization effect when decisiveness is combined with a norm regularization term.

120 This paper also proposes a new self-labeling algorithm for entropy-based clustering. In the context
 121 of relaxed pseudo-labels y , we observe that the standard formulation of decisiveness $\overline{H(y, \sigma)}$ is
 122 sensitive to pseudo-label uncertainty/errors. We motivate the *reverse cross-entropy* formulation,
 123 which we demonstrate is significantly more robust to label noise. We also propose a zero-avoiding
 124 form of KL-divergence as a *strong fairness* term. Unlike standard fairness, it does not tolerate highly
 125 unbalanced clusters. Our new self-labeling loss allows an efficient EM algorithm for estimating
 126 pseudo-labels. We derive closed-form E and M steps. Our new algorithm improves the state-of-the-art
 127 on many standard benchmarks for deep clustering, which empirically validates our technical insights.

128 Our paper is organized as follows. Section 2 discusses the relation of entropy clustering to K-means
 129 and SVM. Section 3 motivates our self-labeling loss and derives an EM algorithm for estimating
 130 pseudo-labels. The experimental results for our entropy clustering algorithm are in Section 4.

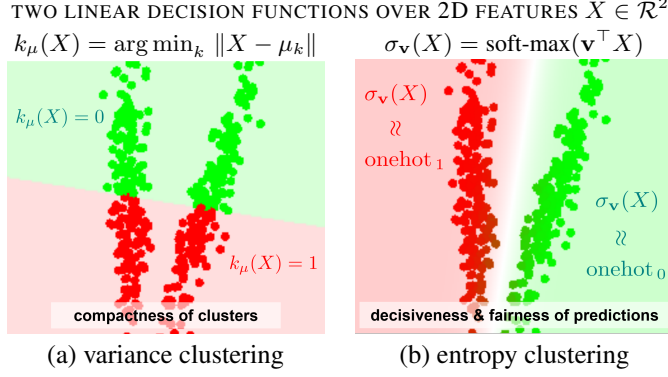


Figure 1: K-means vs entropy clustering - binary example ($K = 2$) for 2D data $\{X_i\} \subset \mathcal{R}^M$ ($M = 2$) comparing linear methods of similar parametric complexity: (a) K -means $[\mu_k \in \mathcal{R}^M]$ and (b) entropy clustering based on a linear classifier using K -columns linear discriminator matrix $\mathbf{v} = [\mathbf{v}_k \in \mathcal{R}^M]$ and soft-max predictions. Red and green colors in (a) and (b) illustrate optimal linear decision regions over $X \in \mathcal{R}^2$ produced by the decision functions $k_\mu(X)$, $\sigma_v(X)$ for parameters μ and \mathbf{v} minimizing two losses: (a) compactness/variance of clusters $\sum_i \|X_i - \mu_{k_i}\|^2$ where $k_i = k_\mu(X_i)$ and (b) decisiveness and fairness of predictions $\overline{H}(\overline{\sigma}) - H(\overline{\sigma})$ where $H(\cdot)$ is entropy function and $\overline{H}(\overline{\sigma}) = \text{avg}\{H(\sigma_i)\}$, $\overline{\sigma} = \text{avg}\{\sigma_i\}$ for $\sigma_i = \sigma_v(X_i)$. The decision function $k_\mu(X)$ is hard (a) and $\sigma_v(X)$ is soft, particularly near the linear decision boundary (b). The optimal results in (a,b) are analyzed in Sec.2.1. The result in (b) may require a *margin maximization* term $\|\mathbf{v}\|^2$, see Sec.2.2.

131 2 Relation to discriminative and generative clustering methods

132 2.1 Entropy-based clustering versus K-means

133 Discriminative entropy clustering (1) is not as widely known as K-means, but for no good reason.
 134 With linear models (3), entropy clustering (1) is as simple as K-means, e.g. it produces linear cluster
 135 boundaries. Both approaches have good approximate optimization algorithms for their non-convex
 136 (1) or NP-hard Mahajan et al. (2012) objectives. Two methods also generalize to non-linear clustering
 137 using more complex representations, e.g. learned $f_w(X)$ or implicit (kernel K-means).

138 There is a limited general understanding of how entropy clustering relates to more popular methods,
 139 such as K-means. The prior work, including Bridle et al. (1991), mainly discusses entropy clustering
 140 in the context of neural networks. K-means is also commonly used with deep features, but it is
 141 hard to understand the differences in such complex settings. An illustrative 2D example of entropy
 142 clustering in Krause et al. (2010) (Fig.1) is helpful, but it looks like a typical textbook example for
 143 K-means where it would work perfectly. Interestingly, Jabi et al. (2021) make a theoretical claim
 144 about algebraic equivalence between K-means objective and a regularized entropy clustering loss.

145 Here we show significant differences between K-means and entropy clustering. First, we disprove
 146 the claim by Jabi et al. (2021). We provide a simple *counterexample* in Figure 1 where the optimal
 147 solutions are different in a basic linear setting. Moreover, we point out a critical technical error in their
 148 Proposition 2 - its proof ignores normalization inside softmax. Symbol \propto hides it in their equation (5),
 149 which is later treated as equality in the proof of Proposition 2. Equations in their proof do not work
 150 with normalization, which is critical for softmax models. The extra regularization term $\|\mathbf{v}\|^2$ in their
 151 entropy loss is also important. Without softmax normalization, $\ln \sigma$ inside cross-entropy $H(y, \sigma)$
 152 turns into a linear term w.r.t. logits $\mathbf{v}^\top x$ and adding $\|\mathbf{v}\|^2$ creates a quadratic form resembling squared
 153 errors $(x - \mathbf{v})^2$ in K-means. In contrast, Section 2.2 shows that regularization $\|\mathbf{v}\|^2$ corresponds to
 154 the *margin maximization* controlling the width of the soft gap between the clusters, see our Fig.1(b).

155 In general, Figure 1 highlights fundamental differences between generative and discriminative
 156 approaches to clustering using two basic linear methods of similar parametric complexity (about
 157 $K \times M$ parameters). K -means (a) seeks balanced compact clusters of the least variance (squared
 158 errors). This can be interpreted “generatively” Kearns et al. (1997) as MLE fitting of two (isotropic)
 159 Gaussian densities, which also explains why K-means fails on highly anisotropic clusters (a). To fix
 160 this “generatively”, one should use non-isotropic Gaussian densities. In particular, 2-mode GMM

161 would produce soft clusters as in (b). But, this increases parametric complexity (two extra covariance
 162 matrices) and leads to quadratic decision boundaries. In contrast, discriminative entropy clustering
 163 in (b) simply looks for the best linear decision boundary giving balanced (“fair”) clusters with data
 164 points away from the boundary (“decisiveness”), regardless of the data density model complexity.

165 2.2 Entropy-based clustering and SVM: margin maximization

166 This section discusses similarities between entropy clustering with soft-max models and unsupervised
 167 SVM methods Ben-Hur et al. (2001); Xu et al. (2004). First, consider the fully supervised setting,
 168 where the relationship between SVMs Vapnik (1995) and logistic regression is known. Assuming
 169 binary classification with target labels $t = \pm 1$, one standard soft-margin SVM loss formulation
 170 combines a margin-maximization term with the *hinge loss* penalizing margin violations, e.g. see
 171 Bishop (2006)

$$L_{svm} = \gamma \|\mathbf{v}\|^2 + \overline{\max\{0, 1 - t \mathbf{v}^\top f\}} \quad (7)$$

172 where the linear classifier norm $\|\mathbf{v}\|$ (excluding bias!) is the reciprocal of the decision margin and
 173 γ is the relative weight of the margin maximization term. For shortness and consistently with the
 174 notation introduced in Sec.1.1, logits $\mathbf{v}^\top f$ include the bias using “homogeneous” representations of
 175 \mathbf{v} and features f , and the “bar” operator represents averaging over all training data points.

176 Instead of the hinge loss, soft-margin maximization (7) can use the *logistic regression* as an alternative
 177 soft penalty for margin violations, see Section 7.1.2 and Figure 7.5 in Bishop (2006),

$$L_{log} = \gamma \|\mathbf{v}\|^2 + \overline{\ln(1 + \exp^{-t \mathbf{v}^\top f})} \equiv \gamma \|\mathbf{v}\|^2 + \overline{H(y, \sigma)} \quad (8)$$

178 where the second *binary cross-entropy* formulation in (8) replaces integer targets $t \in \{\pm 1\}$ with
 179 one-hot target distributions $y \in \{(1, 0), (0, 1)\}$ consistent with our general terminology in Sec.1.2.
 180 Our second formulation in (8) uses soft-max $\sigma = \left\{ \frac{\exp l_1}{\exp l_1 + \exp l_2}, \frac{\exp l_2}{\exp l_1 + \exp l_2} \right\}$ with logits $l_1 = \frac{1}{2} \mathbf{v}^\top f$
 181 and $l_2 = -\frac{1}{2} \mathbf{v}^\top f$; its one advantage is a trivial multi-class generalization. The difference between
 182 the soft-margin maximization losses (7) and (8) is that the flat region of the hinge loss leads to a
 183 sparse set of *support vectors* for the maximum margin solution, see Section 7.1.2 in Bishop (2006).

184 Now, consider the standard SVM-based self-labeling formulation of maximum margin clustering by
 185 Xu et al. (2004). They combine loss (7) with a linear *fairness* constraint $-\epsilon \leq \bar{t} \leq \epsilon$

$$L_{mm} = \gamma \|\mathbf{v}\|^2 + \overline{\max\{0, 1 - t \mathbf{v}^\top f\}}, \quad \text{s.t.} \quad -\epsilon \leq \bar{t} \leq \epsilon \quad (9)$$

186 and treat labels t as optimization variables in addition to model parameters. Note that the hinge loss
 187 encourages consistency between the pseudo labels $t \in \{\pm 1\}$ and the sign of the logits $\mathbf{v}^\top f$. Besides,
 188 loss (9) still encourages maximum margin between the clusters. Keeping data points away from the
 189 decision boundary is similar to the motivation for the *decisiveness* in entropy-based clustering.

190 It is easy to connect (9) to self-labeling entropy clustering. Similarly to (7) and (8), one can replace
 191 the hinge loss by cross-entropy as an alternative margin-violation penalty. As before, the main
 192 difference is that the margin may not be defined by a sparse subset of *support vectors*. We can also
 193 replace the linear balancing constraint in (9) by an entropy-based fairness term. Then, we get

$$L_{semm} = \gamma \|\mathbf{v}\|^2 + \overline{H(y, \sigma)} - H(\bar{y}) \quad (10)$$

194 which is a self-labeling surrogate for the entropy-based maximum-margin clustering loss

$$L_{emm} = \gamma \|\mathbf{v}\|^2 + \overline{H(\sigma)} - H(\bar{\sigma}). \quad (11)$$

195 Losses (11) and (10) are examples of general clustering losses for $K \geq 2$ combining decisiveness and
 196 fairness as in Sections 1.1, 1.2. The first term can be seen as a special case of the norm regularization
 197 in (4). However, instead of a generic model simplicity argument used to justify (4), the specific
 198 combination of cross-entropy with regularizer $\|\mathbf{v}\|^2$ (excluding bias) in (11) and (10) is explicitly
 199 linked to margin maximization where $\frac{1}{\|\mathbf{v}\|}$ corresponds to the margin’s width².

200 It was known that “for a poorly regularized classifier” the combination of decisiveness and fairness
 201 “alone will not necessarily lead to good solutions to unsupervised classification” (Bridle et al. (1991))
 202 and that decision boundary can tightly pass between the data points (Fig.1 in Krause et al. (2010)). The
 203 formal relation to margin maximization above complements such prior knowledge. Our supplementary
 204 material (A) shows the empirical effect of parameter γ in (11) on the inter-cluster gaps.

²The entropy clustering loss (6) is also appended with regularization $\|\mathbf{v}\|^2$ in Jabi et al. (2021), where it is
 incorrectly used for proving K-means connection, see Sec.2.1. They do not discuss margin maximization.

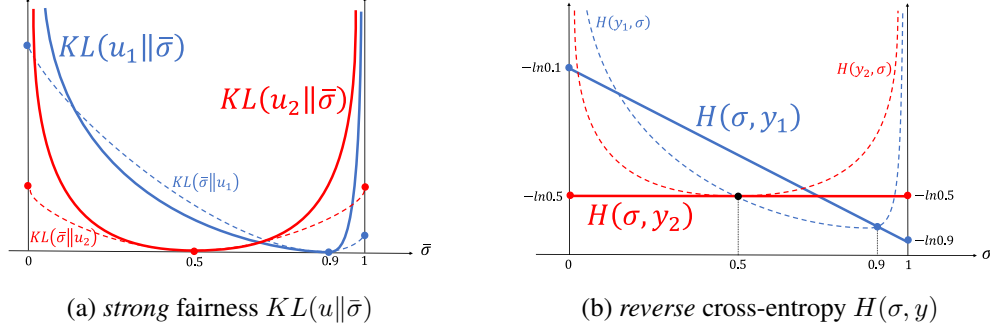


Figure 2: “Forward” vs “reverse”: (a) KL-divergence and (b) cross-entropy. Assuming binary classification $K = 2$, probability distributions σ or $\bar{\sigma}$ are represented as points on $[0,1]$. The solid curves in (a) illustrate the *forward* KL-divergence $KL(u||\bar{\sigma})$ for average predictions $\bar{\sigma}$. We show two examples of volumetric prior $u_1 = (0.9, 0.1)$ (blue) and $u_2 = (0.5, 0.5)$ (red). The reverse KL-divergence $KL(\bar{\sigma}||u)$ (dashed curves), commonly representing fairness in prior work, tolerates extremely unbalanced clustering, i.e. the end points of the interval $[0,1]$. The solid curves in (b) are the *reverse* cross-entropy $H(\sigma, y)$ for predictions σ . The dashed curves are the forward cross-entropy $H(y, \sigma)$. The plots in (b) show examples for two fixed pseudo-labels $y_1 = (0.9, 0.1)$ (blue) and $y_2 = (0.5, 0.5)$ (red). Our loss $H(\sigma, y)$ weakens the training (reduces gradients) on data points with higher label uncertainty (compare blue and red curves). In contrast, the standard loss $H(y, \sigma)$ trains the network to copy this uncertainty, see the optimum σ on the dashed curves. The boundedness of $H(\sigma, y)$ also represents robustness to errors in y .

205 3 Our self-labeling entropy clustering method

206 The conceptual properties discussed in the previous section may improve the general understanding
 207 of entropy clustering, but their new practical benefits are limited. For example, margin maximization
 208 implicitly happens in prior entropy methods since norm regularization (weight-decay) is omnipresent.

209 This section addresses some specific limitations of prior entropy clustering formulations that do
 210 affect the practical performance. We focus on self-labeling (Sec.1.2) and observe that the standard
 211 cross-entropy formulation of decisiveness is sensitive to pseudo-label errors. Section 3.1 introduces
 212 our new self-labeling loss using the *reverse cross-entropy*, which we show is more robust to label
 213 noise. We also propose *strong fairness*. Section 3.2 derives an efficient EM algorithm for minimizing
 214 our loss w.r.t. pseudo-labels, which is a critical step of our self-labeling algorithm.

215 3.1 Our self-labeling loss formulation

216 We start from the maximum-margin entropy clustering (10) where the entropy fairness can be replaced
 217 by an equivalent KL-divergence term explicitly expressing the target balance distribution u . This
 218 gives a self-labeling variant of the loss (4) in Krause et al. (2010) similar to (6) in Jabi et al. (2021)

$$L_{semm} \stackrel{c}{=} \overline{H(y, \sigma)} + KL(\bar{y} || u) + \gamma \|\mathbf{v}\|^2. \quad (12)$$

219 We propose two changes to this loss based on several numerical insights leading to a significant
 220 performance improvement over Krause et al. (2010) and Jabi et al. (2021). First, we reverse the order
 221 of the cross-entropy arguments, see Fig.2(b). This improves the robustness of network predictions σ
 222 to errors in estimated pseudo-labels y , as confirmed by our experiment in Figure 3. This reversal also
 223 works for estimating pseudo-labels y as the second argument in cross-entropy is a standard position
 224 for an “estimated” distribution. Second, we also observe that the standard fairness term in (12,4,6)
 225 is the *reverse* KL divergence w.r.t. cluster volumes, i.e. the average predictions $\bar{\sigma}$. It can tolerate
 226 highly unbalanced solutions where $\bar{\sigma}_k = 0$ for some cluster k , see the dashed curves in Fig.2(a). We
 227 propose the *forward*, a.k.a. *zero-avoiding*, KL divergence $KL(u || \bar{\sigma})$, see the solid curves Fig.2(a). We
 228 refer to this as *strong fairness*.

229 The two changes above modify the clustering loss (12) into our formulation of self-labeling loss

$$L_{our} := \overline{H(\sigma, y)} + \lambda KL(u || \bar{y}) + \gamma \|\mathbf{v}\|^2. \quad (13)$$

230 3.2 Our EM algorithm for pseudo-labels

231 Minimization of a self-supervised loss w.r.t pseudo-labels y for given predictions σ is a critical operation in iterative self-labeling techniques Asano et al. (2020); Jabi et al. (2021), see Sec.1.2. Besides well-motivated numerical properties of our new loss (13), in practice it also matters that it has an efficient solver for pseudo-labels. While (13) is convex w.r.t. y , optimization is done over a probability simplex and a good practical solver is not given. Note that $H(\sigma, y)$ works as a *log barrier* for the constraint $y \in \Delta^K$. This could be problematic for the first-order methods, but a basic Newton’s method is a good match, e.g. Kelley (1995). The overall convergence rate of such second-order methods is fast, but computing the Hessian’s inverse is costly, see Table 1. Instead, we derive a more efficient *expectation-maximization* (EM) algorithm.

248 Assume that model parameters and predictions in (13) are fixed, i.e. \mathbf{v} and σ . Following *variational inference* Bishop (2006), we introduce K auxiliary latent variables, distributions $S^k \in \Delta^N$ representing normalized support of each cluster k over N data points. In contrast, N distributions $y_i \in \Delta^K$ show support for each class at every point X_i . We refer to each vector S^k as a *normalized cluster k* . Note that here we focus on individual data points and explicitly index them by $i \in \{1, \dots, N\}$. Thus, we use $y_i \in \Delta^K$ and $\sigma_i \in \Delta^K$. Individual components of distribution $S^k \in \Delta^N$ corresponding to data point X_i is denoted by scalar S_i^k .

258 First, we expand our loss (13) using our new latent variables $S^k \in \Delta^N$

$$L_{our} \stackrel{c}{=} \overline{H(\sigma, y)} + \lambda H(u, \bar{y}) + \gamma \|\mathbf{v}\|^2 \quad (14)$$

$$\begin{aligned} &= \overline{H(\sigma, y)} - \lambda \sum_k u^k \ln \sum_i S_i^k \frac{y_i^k}{S_i^k N} + \gamma \|\mathbf{v}\|^2 \\ &\leq \overline{H(\sigma, y)} - \lambda \sum_k \sum_i u^k S_i^k \ln \frac{y_i^k}{S_i^k N} + \gamma \|\mathbf{v}\|^2 \end{aligned} \quad (15)$$

259 Due to the convexity of negative log, we apply Jensen’s inequality to derive an upper bound, i.e. (15), to L_{our} . Such a bound becomes tight when:

$$\text{E-step :} \quad S_i^k = \frac{y_i^k}{\sum_j y_j^k} \quad (16)$$

261 Then, we fix S_i^k as (16) and solve the Lagrangian of (15) with simplex constraint to update y as:

$$\text{M-step :} \quad y_i^k = \frac{\sigma_i^k + \lambda N u^k S_i^k}{1 + \lambda N \sum_c u^c S_i^c} \quad (17)$$

262 We run these two steps until convergence with respect to some predefined tolerance. Note that the minimum y is guaranteed to be globally optimal since (14) is convex w.r.t. y . The empirical convergence rate is within 15 steps on MNIST. The comparison of computation speed on synthetic data is shown in Table 1. While the number of iterations to convergence is roughly the same as Newton’s methods, our EM algorithm is much faster in terms of running time and is extremely easy to implement using the highly optimized built-in functions from the standard PyTorch library that supports GPU.

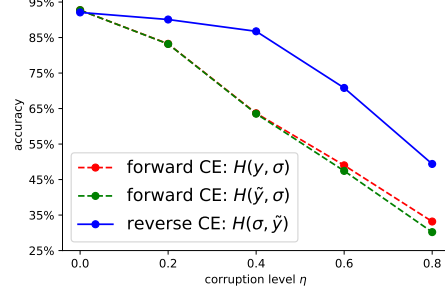


Figure 3: Robustness to noisy labels: reverse $H(\sigma, y)$ vs standard cross-entropy $H(y, \sigma)$. We train ResNet-18 on fully-supervised *Natural Scene* dataset [NSD] where we corrupted some labels. The horizontal axis shows the corruption level, i.e. percentage η of training images where correct ground truth labels were replaced by a random label. We use soft target distributions $\tilde{y} = \eta * u + (1 - \eta) * y$ that is a mixture of one-hot distribution y for the observed corrupt label and the uniform distribution u , as in Müller et al. (2019). The vertical axis shows the test accuracy. Reverse cross-entropy improves robustness to high labeling errors.

K	number of iterations (to convergence)			running time in sec. (to convergence)		
	2	20	200	2	20	200
Newton	3	3	4	$2.8e^{-2}$	$3.3e^{-2}$	$1.7e^{-1}$
EM	2	2	2	$9.9e^{-4}$	$2.0e^{-3}$	$4.0e^{-3}$

Table 1: Our EM algorithm vs Newton’s methods Kelley (1995).

272 Inspired by Springenberg (2015); Hu et al. (2017), we also adapted our EM algorithm to allow
 273 for updating y within each batch. In fact, the mini-batch approximation of (14) is an upper bound.
 274 Considering the first two terms of (14), we can use Jensen’s inequality to get:

$$\overline{H(\sigma, y)} + \lambda H(u, \bar{y}) \leq \mathbb{E}_B[\overline{H_B(\sigma, y)} + \lambda H(u, \bar{y}_B)] \quad (18)$$

275 where B is the batch randomly sampled from the whole dataset. Now, we can apply our EM algorithm
 276 to update y in each batch, which is even more efficient. Compared to other methods Ghasedi Dizaji
 277 et al. (2017); Asano et al. (2020); Jabi et al. (2021) which also use the auxiliary variable y , we can
 278 efficiently update y on the fly while they only update once or just a few times per epoch due to the
 279 inefficiency to update y for the whole dataset per iteration. Interestingly, we found that it is actually
 280 important to update y on the fly, which makes convergence faster and improves the performance
 281 significantly (see supplementary material). We use this “batch version” EM throughout all the
 282 experiments. Our full algorithm for the loss (13) is summarized in supplementary material.

283 4 Experimental results

284 Our experiments start from clustering on fixed features to joint training with feature learning. We test
 285 our approach on standard benchmark datasets with different network architectures. We also provide
 286 the comparison of different losses under weakly-supervised settings (see supplementary material).

287 **Dataset** For the clustering problem, we use four standard benchmark datasets: MNIST Lecun et al.
 288 (1998), CIFAR10/100 Torralba et al. (2008) and STL10 Coates et al. (2011). We follow Ji et al.
 289 (2019) to use the whole dataset for training and testing unless otherwise specified.

290 **Evaluation** As for the evaluation on clustering, we set the number of clusters to the number
 291 of ground-truth category labels and adopt the standard method Kuhn (1955) by finding the best
 292 one-to-one mapping between clusters and labels.

293 4.1 Clustering with fixed features

294 We compare our method against the state-of-the-art methods using fixed deep features generated by
 295 pre-trained (ImageNet) ResNet-50 He et al. (2016). We use a one-layer linear classifier for all losses
 296 except for K-means. We set λ in our loss to 100. We use stochastic gradient descent with learning rate
 297 0.1 to optimize the loss for 10 epochs. The batch size was set to 250. The coefficients for the margin
 298 maximization terms are set to 0.001, 0.02, 0.009, and 0.02 for MNIST, CIFAR10, CIFAR100 and
 299 STL10 respectively. As stated in Section 2.2, such coefficient is important for the optimal decision
 300 boundary, especially when features are fixed. If we simultaneously learn the representation/feature
 301 and cluster the data, we observed that the results are less sensitive to such coefficient.

	STL10	CIFAR10	CIFAR100 (20)	MNIST
K-means	85.20%(5.9)	67.78%(4.6)	42.99%(1.3)	47.62%(2.1)
MI-GD Bridle et al. (1991); Krause et al. (2010)	89.56%(6.4)	72.32%(5.8)	43.59%(1.1)	52.92%(3.0)
SeLa Asano et al. (2020)	90.33%(4.8)	63.31%(3.7)	40.74%(1.1)	52.38%(5.2)
MI-ADM Jabi et al. (2021)	81.28%(7.2)	56.07%(5.5)	36.70%(1.1)	47.15%(3.7)
MI-ADM* Jabi et al. (2021)	88.64%(7.1)	60.57%(3.3)	41.2%(1.4)	50.61%(1.3)
Our	92.2%(6.2)	73.48%(6.2)	43.8%(1.1)	58.2%(3.1)

Table 2: Comparison of different methods using fixed features. The numbers are the average accuracy and the standard deviation over 6 trials. *: our “batch version” implementation of their method.

302 4.2 Joint clustering and feature learning

303 In this section, we train a deep network to jointly learn the features and cluster the data. We test our
 304 method on both a small architecture (VGG4) and a large one (ResNet-18). The only extra standard
 305 technique we add here is the self-augmentation, following Hu et al. (2017); Ji et al. (2019); Asano
 306 et al. (2020). The experimental settings and more details are given in the supplementary material.

307 To train the VGG4, we use random initialization for network parameters. From Table 3, it can
 308 be seen that our approach consistently achieves the most competitive results in terms of accuracy

309 (ACC). Most of the methods we compared in our work (including our method) are general concepts
 310 applicable to single-stage end-to-end training. To be fair, we tested all of them on the same simple
 311 architecture. But, these general methods can be easily integrated into other more complex systems.

	STL10	CIFAR10	CIFAR100 (20)	MNIST
MI-D* Hu et al. (2017)	25.28%(0.5)	21.4%(0.5)	14.39%(0.7)	92.90%(6.3)
IIC* Ji et al. (2019)	24.12%(1.7)	21.3%(1.4)	12.58%(0.6)	82.51%(2.3)
SeLa [§] Asano et al. (2020)	23.99%(0.9)	24.16%(1.5)	15.34%(0.3)	52.86%(1.9)
MI-ADM [§] Jabi et al. (2021)	17.37%(0.9)	17.27%(0.6)	11.02%(0.5)	17.75%(1.3)
MI-ADM ^{*,§} Jabi et al. (2021)	23.37%(0.9)	23.26%(0.6)	14.02%(0.5)	78.88%(3.3)
Our ^{*,§}	25.33%(1.4)	24.16%(0.8)	15.09%(0.5)	93.58%(4.8)

Table 3: Quantitative results of accuracy for unsupervised clustering methods with VGG4. We only use the 20 coarse categories for CIFAR100. We reuse the code published by Ji et al. (2019); Asano et al. (2020); Hu et al. (2017) and implemented the optimization for loss of Jabi et al. (2021) according to the paper. *: all variables are updated for each batch. §: loss formula has pseudo-label.

312 As for the training of ResNet-18, we found that random initialization does not work well when we only
 313 use self-augmentation. We may need more training tricks such as auxiliary over-clustering, multiple
 314 heads, and more augmentations Ji et al. (2019). In the mean time, the authors from Van Gansbeke
 315 et al. (2020) proposed a three-stage approach for the unsupervised classification and we found that
 316 the pre-trained weight from their first stage is beneficial to us. For a fair comparison, we followed
 317 their experimental settings and compared ours to their second-stage results. Note that they split the
 318 data into training and testing. We also report two additional evaluation metrics, i.e. NMI and ARI.

319 In Table 4, we show the results using their pretext-trained network (stage one) as initialization for
 320 our entropy clustering. We use only our clustering loss together with the self-augmentation (one
 321 augmentation per image this time) to reach higher numbers than SCAN, as shown in the table below.

	CIFAR10			CIFAR100 (20)			STL10		
	ACC	NMI	ARI	ACC	NMI	ARI	ACC	NMI	ARI
SCAN Van Gansbeke et al. (2020)	81.8 (0.3)	71.2 (0.4)	66.5 (0.4)	42.2 (3.0)	44.1 (1.0)	26.7 (1.3)	75.5 (2.0)	65.4 (1.2)	59.0 (1.6)
Our	83.09 (0.2)	71.65 (0.1)	68.05 (0.1)	46.79 (0.3)	43.27 (0.1)	28.51 (0.1)	77.67 (0.1)	67.66 (0.3)	61.26 (0.4)

Table 4: Quantitative comparison using network ResNet-18.

322 5 Conclusions

323 Our paper proposed a new self-labeling algorithm for discriminative entropy clustering, but we
 324 also clarify several important conceptual properties of this general methodology. For example, we
 325 disproved a theoretical claim in a recent TPAMI paper stating the equivalence between variance
 326 clustering (K-means) and discriminative entropy-based clustering. We also demonstrate that standard
 327 formulations of entropy clustering losses may lead to narrow decision margins. Unlike prior work on
 328 discriminative entropy clustering, we show that classifier norm regularization is important for margin
 329 maximization.

330 We also discussed several limitations of the existing self-labeling formulations of entropy clustering
 331 and propose a new loss addressing such limitations. In particular, we replace the standard (forward)
 332 cross-entropy by the *reverse cross-entropy* that we show is significantly more robust to errors in esti-
 333 mated soft pseudo-labels. Our loss also uses a strong formulation of the fairness constraint motivated
 334 by a *zero-avoiding* version of KL divergence. Moreover, we designed an efficient EM algorithm
 335 minimizing our loss w.r.t. pseudo-labels; it is significantly faster than standard alternatives, e.g
 336 Newton’s method. Our empirical results improved the state-of-the-art on many standard benchmarks
 337 for deep clustering.

338 **References**

- 339 Asano, Y. M., Rupprecht, C., and Vedaldi, A. Self-labelling via simultaneous clustering and
340 representation learning. In *International Conference on Learning Representations*, 2020.
- 341 Ben-Hur, A., Horn, D., Siegelman, H., and Vapnik, V. Support vector clustering. *Journal of Machine*
342 *Learning Research*, 2:125 – 137, 2001.
- 343 Bishop, C. M. *Pattern Recognition and Machine Learning*. Springer, 2006.
- 344 Bridle, J. S., Heading, A. J. R., and MacKay, D. J. C. Unsupervised classifiers, mutual information
345 and 'phantom targets'. In *NIPS*, pp. 1096–1101, 1991.
- 346 Coates, A., Ng, A., and Lee, H. An analysis of single-layer networks in unsupervised feature learning.
347 In *Proceedings of the fourteenth international conference on artificial intelligence and statistics*,
348 pp. 215–223. JMLR Workshop and Conference Proceedings, 2011.
- 349 Cuturi, M. Sinkhorn distances: Lightspeed computation of optimal transport. *Advances in neural*
350 *information processing systems*, 26, 2013.
- 351 Ghasedi Dizaji, K., Herandi, A., Deng, C., Cai, W., and Huang, H. Deep clustering via joint
352 convolutional autoencoder embedding and relative entropy minimization. In *Proceedings of the*
353 *IEEE international conference on computer vision*, pp. 5736–5745, 2017.
- 354 Grandvalet, Y. and Bengio, Y. Semi-supervised learning by entropy minimization. *Advances in*
355 *neural information processing systems*, 17, 2004.
- 356 Guo, C., Pleiss, G., Sun, Y., and Weinberger, K. Q. On calibration of modern neural networks. In
357 *International conference on machine learning*, pp. 1321–1330. PMLR, 2017.
- 358 He, K., Zhang, X., Ren, S., and Sun, J. Deep residual learning for image recognition. In *Proceedings*
359 *of the IEEE conference on computer vision and pattern recognition*, pp. 770–778, 2016.
- 360 Hu, W., Miyato, T., Tokui, S., Matsumoto, E., and Sugiyama, M. Learning discrete representations
361 via information maximizing self-augmented training. In *International conference on machine*
362 *learning*, pp. 1558–1567. PMLR, 2017.
- 363 Jabi, M., Pedersoli, M., Mitiche, A., and Ayed, I. B. Deep clustering: On the link between discrimi-
364 native models and k-means. *IEEE Transactions on Pattern Analysis and Machine Intelligence*, 43
365 (6):1887–1896, 2021.
- 366 Ji, X., Henriques, J. F., and Vedaldi, A. Invariant information clustering for unsupervised image
367 classification and segmentation. In *Proceedings of the IEEE/CVF International Conference on*
368 *Computer Vision*, pp. 9865–9874, 2019.
- 369 Kearns, M., Mansour, Y., and Ng, A. Y. An information-theoretic analysis of hard and soft assignment
370 methods for clustering. In *UAI '97: Proceedings of the Thirteenth Conference on Uncertainty in*
371 *Artificial Intelligence, Brown University, Providence, Rhode Island, USA, August 1-3, 1997*, pp.
372 282–293. Morgan Kaufmann, 1997.
- 373 Kelley, C. T. *Iterative methods for linear and nonlinear equations*. SIAM, 1995.
- 374 Krause, A., Perona, P., and Gomes, R. Discriminative clustering by regularized information maxi-
375 mization. *Advances in neural information processing systems*, 23, 2010.
- 376 Kuhn, H. W. The hungarian method for the assignment problem. *Naval research logistics quarterly*,
377 2(1-2):83–97, 1955.
- 378 Lecun, Y., Bottou, L., Bengio, Y., and Haffner, P. Gradient-based learning applied to document
379 recognition. *Proceedings of the IEEE*, 86(11):2278–2324, 1998.
- 380 Mahajan, M., Nimbhorkar, P., and Varadarajan, K. The planar K-means problem is NP-hard.
381 *Theoretical Computer Science*, 442:13–21, 2012.
- 382 Müller, R., Kornblith, S., and Hinton, G. E. When does label smoothing help? *Advances in neural*
383 *information processing systems*, 32, 2019.

- 384 NSD. Natural Scenes Dataset [NSD]. [https://www.kaggle.com/datasets/
385 nitishabharathi/scene-classification](https://www.kaggle.com/datasets/nitishabharathi/scene-classification), 2020.
- 386 Pereyra, G., Tucker, G., Chorowski, J., Kaiser, Ł., and Hinton, G. Regularizing neural networks by
387 penalizing confident output distributions. *ICLR workshop, arXiv:1701.06548*, 2017.
- 388 Rumelhart, D. E., Hinton, G. E., and Williams, R. J. Learning representations by back-propagating
389 errors. *Nature*, 323(6088):533–536, 1986.
- 390 Song, H., Kim, M., Park, D., Shin, Y., and Lee, J.-G. Learning from noisy labels with deep neural
391 networks: A survey. *IEEE Transactions on Neural Networks and Learning Systems*, 2022.
- 392 Springenberg, J. T. Unsupervised and semi-supervised learning with categorical generative adversarial
393 networks. In *International Conference on Learning Representations*, 2015.
- 394 Tanaka, D., Ikami, D., Yamasaki, T., and Aizawa, K. Joint optimization framework for learning with
395 noisy labels. In *Proceedings of the IEEE conference on computer vision and pattern recognition*,
396 pp. 5552–5560, 2018.
- 397 Torralba, A., Fergus, R., and Freeman, W. T. 80 million tiny images: A large data set for nonparametric
398 object and scene recognition. *IEEE transactions on pattern analysis and machine intelligence*, 30
399 (11):1958–1970, 2008.
- 400 Van Gansbeke, W., Vandenhende, S., Georgoulis, S., Proesmans, M., and Van Gool, L. Scan: Learning
401 to classify images without labels. In *Computer Vision—ECCV 2020: 16th European Conference,
402 Glasgow, UK, August 23–28, 2020, Proceedings, Part X*, pp. 268–285. Springer, 2020.
- 403 Vapnik, V. *The Nature of Statistical Learning Theory*. Springer, 1995.
- 404 Xu, L., Neufeld, J., Larson, B., and Schuurmans, D. Maximum margin clustering. In Saul, L., Weiss,
405 Y., and Bottou, L. (eds.), *Advances in Neural Information Processing Systems*, volume 17. MIT
406 Press, 2004.